Excess radiation exacerbates drought stress impacts on canopy conductance along aridity gradients

Jing Wang[1], Xuefa Wen[1,2,3,4]

[1]Key Laboratory of Ecosystem Network Observation and Modeling, Institute of Geographic Sciences and Natural Resources Research, Chinese Academy of Sciences, Beijing, 100101, China
[2]Collaborative Innovation Center on Forecast and Evaluation of Meteorological Disasters (CIC-FEMD), Nanjing University of Information Science and Technology, Nanjing, China
[3]College of Resources and Environment, University of Chinese Academy of Sciences, Beijing, 101408, China
[4]Beijing Yanshan Earth Critical Zone National Research Station, University of Chinese Academy of Sciences, Beijing, 101408, China

Correspondence to: Xuefa Wen (wenxf@igsnrr.ac.cn) and Jing Wang (wangjing.15b@igsnrr.ac.cn)

Abstract. Stomatal conductance (g_s) of all co-existing species regulates transpiration in arid and semi-arid grasslands prone to droughts. However, the effect of drought stress on canopy conductance (G_s) is debated, and the interactive effects of abiotic and biotic constraints on G_s remain poorly understood. Here, we used ^{18}O enrichment above source water ($\triangle^{18}O$) of leaf organic matter as a proxy for G_s to increase understanding of these effects. Three grassland transects were established along aridity gradients in Loess Plateau (LP), Inner Mongolian Plateau (MP), and Tibetan Plateau (TP) which differ in solar radiation and temperature conditions. Results showed that G_s consistently decreased with increasing aridity within transects. G_s in TP was lower than that in the other two plateaus for a given level of aridity due to low temperature and high radiation. The primary determinant of drought stress on G_s was soil moisture (SM) in LP and MP, and vapor pressure deficit (VPD) in TP. Solar radiation exhibited a consistently negative effect on G_s via drought stress within transects, while temperature had negative effects on G_s in TP, and no effects in LP and MP. Adding the interaction of leaf area and abiotic factors increases the percent of explained variability in G_s by 17 and 36% in LP and MP, respectively, but not in TP, where climate exerts an overwhelming effect. These results highlighted the need to integrate multiple stressors and plant properties to determine spatial variability in G_s.

Keywords: stomatal conductance, oxygen isotope, drought stress, excess radiation, high temperature, grassland

1 Introduction

Stomatal conductance (g_s) of all co-existing species plays a significant role in water loss (transpiration) and carbon uptake (photosynthesis) at an ecosystem level, thereby coupling water and carbon cycles (Jarvis and McNaughton 1986; Martin-StPaul *et al.* 2017). Model linkages between g_s at species level and photosynthesis indicate that the biophysical response of g_s at species level varies depending on water, radiation, temperature, and leaf economic traits (Buckley 2019; Farquhar *et al.* 1980; Leuning 1995; Wright *et al.* 2004). However, experimental evidence suggested that the strength of g_s at species level

responses to changing environmental factors varies with species (Galmes *et al.* 2007), and changes in environmental factors can have interactive effects on the variability in g_s at species level (Costa *et al.* 2015; Doupis *et al.* 2020; Zeuthen *et al.* 1997). Plant communities are simultaneously affected in the field by a variety of environmental stressors, and canopy conductance (G_s) is the cumulative rate over time of co-occurring species (Xia *et al.*, 2015). However, how interactive effects of multiple environmental stressors and community traits regulate the spatial patterns in G_s remains largely unknown.

Drylands cover 41% of the Earth's surface (Yao *et al.* 2020) and drive the variability in global terrestrial carbon sink (Ahlstrom *et al.* 2015). The survival, transpiration, and productivity of plants growing in dry areas are simultaneously stressed by drought, high solar radiation, and temperature (Peguero-Pina *et al.* 2020). In addition, communities respond to drought, solar radiation, and temperature stressors by changing their functional traits (Fyllas *et al.* 2017; Martin-StPaul *et al.* 2017); this may ultimately affect G_s. Thus, G_s in drylands was expected to be influenced by the interaction of drought, high radiation, high temperature, and biotic factors.

G_s should be primarily limited in drylands by drought, which is often characterized by low soil moisture (SM) and high vapor pressure deficit (VPD) (Liu *et al.* 2020). The limitation of SM and VPD on g_s at species level involves two independent mechanisms: (1) low SM (available water in the soil for plant root uptake) reduces soil water potential and hinders the transport of soil water to leaf; (2) high VPD reduces leaf water potential and increases transpiration demand (Buckley 2019; Oren *et al.* 1999). However, there is an ongoing debate on the relative role of SM and VPD in determining the response of G_s to drought (Kimm *et al.* 2020; Liu *et al.* 2020; Novick *et al.* 2016). For instance, a global analysis demonstrated that SM stress is the dominant driver of G_s in xeric ecosystems (Novick *et al.* 2016). However, another study demonstrated that the variability in Gs in rain-fed maize and soybean over a precipitation gradient (283 mm to 683 mm per growing season) was mainly determined by VPD stress (Kimm *et al.* 2020).

Solar radiation and temperature may directly regulate G_s (Buckley 2019; Farquhar *et al.* 1980; Leuning 1995) and adjust drought stress (Costa *et al.* 2015; Doupis *et al.* 2020; Zeuthen *et al.* 1997). However, previous studies showed that the effects of direction and intensity of solar radiation and temperature on gs at species level strongly depend on their distribution range and the relationship with aridity. For example, the response of g_s at species level to solar radiation and temperature generally shows an increasing trend up to optimum values (Xu *et al.* 2021a), while excess radiation (Costa *et al.* 2015; Doupis *et al.* 2020; Zeuthen *et al.* 1997) and high temperature-associated high VPD or low SM (Seneviratne *et al.* 2010) would suppress g_s. However, these effects were obscured by drought stress in natural conditions, which alone caused a gs at species level reduction (Duan *et al.* 2008; Fu *et al.* 2006). Consequently, it is difficult to disentangle whether the decline in G_s with increasing aridity is simply a consequence of drought stress or interaction of multiple stressors.

Given that gs and photosynthesis at species level are closely correlated (Leuning 1995), environmental stressors should have an indirect effect on G_s by regulating community morphological traits. However, few studies have addressed this topic at the community scale considering both environmental and plant regulators (Wang and Wen 2022a, b, c). Communities

change their morphological functional traits to tolerate environmental stress, including leaf area (LA) and specific leaf area (SLA) (Wright *et al.* 2017). LA and SLA determine plant capacity for capturing light (Poorter *et al.* 2009), leaf heat exchange (Wright *et al.* 2017), and length of water pathway through leaves (Kang *et al.* 2021), all of which are closely related to transpiration and photosynthesis. Previous studies focused primarily on the patterns of LA and SLA along environmental gradients (Peppe *et al.* 2011; Wright *et al.* 2017). For example, small-leaved species prevail in dry, hot, sunny environments, or at high elevations (Wright *et al.* 2017). SLA generally decreases with increasing radiation and drought stress, and increases with decreases in temperature (Poorter *et al.*, 2009). Recently, a study conducted in woody species in eastern Qinghai-Tibet, China, showed that LA and stomatal size co-varied with temperature (Kang *et al.* 2021), indicating that the changes in LA and SLA may play important roles in regulating G_s.

To investigate the interactive effect of environmental stressors and biotic factors on G_s, three grassland transects were established along aridity gradients, one in Loess Plateau (LP), one in Mongolian Plateau (MP), and one in Tibetan Plateau (TP) in an arid and semi-arid region in China. The grassland transects span gradients of precipitation, SM, VPD, solar radiation, and temperature, and provide an ideal platform for exploration of interactive effects of multiple stressors and biotic factors on G_s (Table S1). In addition, the three grassland transects experience different solar radiation and temperature conditions at a given aridity, due to the differences in geographical locations of the three plateaus. The order of mean annual temperature and solar radiation across the sites is LP>MP>TP and LP<MP<TP, respectively. We hypothesized that: (1) increasing solar radiation and/or air temperature along the aridity gradient will exacerbate drought stress impacts on G_s within transects, (2) high solar radiation and low temperatures will jointly suppress G_s at a given aridity among transects, and (3) integrating environmental stress and community functional traits will significantly improve the capacity for predicting G_s. To test our hypotheses, time-integrated G_s was represented by community-weighted ^{18}O enrichment above source water of leaf organic matter ($\triangle^{18}O$) (Cabrera *et al.* 2021; Hirl *et al.* 2021).

2 Materials and methods

2.1 Study areas

In this study, we established three grassland transects spanning a broad range of climatic conditions and grassland types in arid and semi-arid regions (i.e., Loess Plateau, LP; Inner Mongolian Plateau, MP; Tibetan Plateau, TP) in China (Lyu *et al.* 2021). Transects were 600 km long in LP, 1200 km in MP, and 1500 km in TP. In each transect, we selected 10 sampling sites with increasing aridity from east to west (calculated as 1- mean annual precipitation/potential evapotranspiration). Solar radiation and growing season vapor pressure deficit (VPD) increased, and growing season soil moisture (SM) decreased with increasing aridity (Supplementary 1-Table S1). Among transects, differences in aridity (Fig.1a), precipitation (Fig.1b and Fig.S1a; Table S2), growing season SM (Fig.1c), community leaf area (Fig.1h) and leaf specific leaf area (SLA) (Fig.1i) were not significant ($P>0.05$), while differences in VPD (Fig.1d and Fig.S1b; Table S2), solar radiation (SR) (Fig.1e and Fig.S1c; Table S2), and

air temperature (Fig.1f and Fig.S1d; Table S2) were significant. More details about the characteristics of climate, soil and vegetation type in the 30 sampling sites can be found in Lyu *et al.* (2021).

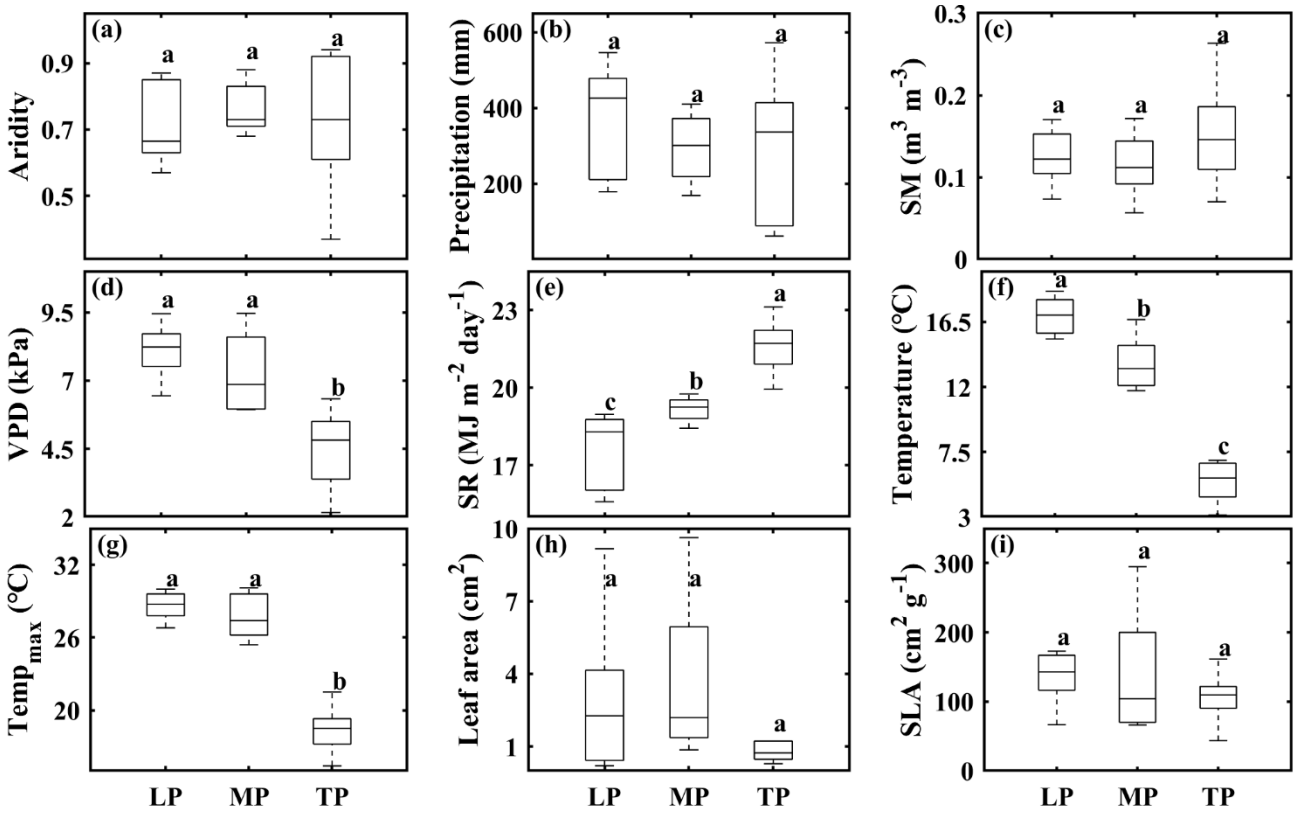

Figure 1. Comparison of aridity (a), growing season precipitation (b), soil moisture (SM) (c), vapor pressure deficit (VPD) (d), solar radiation (SR) (e), temperature (f), maximum temperature ($Temp_{max}$) (g), community leaf area (h), and specific leaf area (SLA) (i) among transects. LP: Loess Plateau; MP, Inner Mongolia Plateau; TP, Tibetan Plateau. Lowercase letters indicate significant differences among transects ($P<0.05$). Error bars indicate standard error of the mean; n=10.

2.2 Sampling and measurements

2.2.1 Sample processing

A field survey and sample collection were conducted during the peak growing season (July to August) in 2018. Within each of 30 sites, we delineated eight 1m × 1m plots in a 100m x 100m sampling area. Plant species (identified by experienced plant taxonomists), the number of species, and community structure were surveyed (Supplementary 2). Aboveground biomass was collected by species for dry mass and stable isotope analyses.

2.2.2 Leaf area and SLA analysis

Three individuals per site were collected as replications for each species, and six to ten fresh, healthy, and mature leaves were selected from individuals of each species for leaf area (LA) determination with a portable scanner (Cano Scan LIDE 110, Japan). Image J software was used to obtain LA values (Schneider *et al.*, 2012). Then, leaves were dried at 60℃ and weighed for leaf dry mass. SLA was calculated by dividing LA by leaf dry mass. Dried leaf samples were ground using a ball mill, and oven dried before $\delta^{18}O$ analysis.

2.2.3 Stable isotope analysis

An isotope ratio mass spectrometer in continuous-flow mode (Model 253 plus, Thermo Fisher Scientific, Bremen, Germany) coupled with an elemental analyzer (Model Flash 2000HT, Thermo Fisher Scientific, Bremen, Germany) was used to determine $\delta^{18}O$ values (Wang *et al.* 2021a; Wang *et al.* 2021b). Isotope ratios are expressed as per mil deviations relative to VSMOW (oxygen) standards. Long-term precision for the instrument was < 0.2‰ for $\delta^{18}O$ measurements. Leaf $\delta^{18}O$ at species level ranged from 12.07 to 35.35‰ in LP, 17.42 to 32.65‰ in MP, and 12.07 to 35.35‰ in TP (Table S3; Fig.S2).

We expressed observed leaf $\delta^{18}O$ as $\triangle^{18}O$ at species level ($\triangle^{18}O_L$) to remove the source-water effects on leaf $\delta^{18}O$ (Guerrieri *et al.* 2019; Helliker and Richter 2008; Maxwell *et al.* 2018):

$$\triangle^{18}O_L = \frac{(\delta^{18}O_L - \delta^{18}O_S)}{(1+\delta^{18}O_S/1000)} \qquad (1)$$

where $\delta^{18}O_L$ and $\delta^{18}O_S$ is the $\delta^{18}O$ of bulk-leaf at species level and source water, respectively. Generally, data on long-term stem water isotopic composition in each species are not available. As precipitation is the only or the main source of water in dryland ecosystems, we assumed that the amount-weighted $\delta^{18}O$ of precipitation during the growing season can reflect $\delta^{18}O$ of source water (Guerrieri *et al.* 2019; Maxwell *et al.* 2018). $\delta^{18}O$ of monthly precipitation at each site was simulated using longitude, latitude, and elevation according to (Bowen *et al.* 2005). $\triangle^{18}O$ at species level ranged from 21.69 to 43.89‰ in LP, 24.68 to 41.68‰ in MP, and 21.69 to 43.89‰ in TP (Table S3; Fig.S2).

Given that leaf $\delta^{18}O$ at species level is affected by the leaf water evaporation process, variability in stomatal conductance (g_s) is expected to be evident in leaf $\delta^{18}O$ (Barbour 2007; Barbour and Farquhar 2000; Farquhar *et al.* 1998). A negative relationship between $\triangle^{18}O$ and gs has been observed at species (Barbour and Farquhar 2000; Cabrera-Bosquet *et al.* 2011; Grams *et al.* 2007; Moreno-Gutierrez *et al.* 2012) and canopy scales (Cabrera *et al.* 2021; Hirl *et al.* 2021), and among communities along soil (Ramirez *et al.* 2009) and climatic (Keitel *et al.* 2006) gradients. Consequently, we selected $1/\triangle^{18}O$ to be used as proxy for g_s at species level in this study.

2.3 Community $1/\triangle^{18}O$, LA, and SLA

Plant community parameters ($1/\triangle^{18}O$, LA, and SLA) were defined for each sampling site, and calculated as an average of eight quadrats. The $1/\triangle^{18}O$, LA, and SLA were scaled from leaf to community levels as follows:

$$1/\triangle^{18}O=\sum_{n}^{i} BF_i \times (1/\triangle^{18}O_L)_i \quad (2)$$

$$LA=\sum_{n}^{i} BF_i \times (LA_L)_i \quad (3)$$

$$SLA=\sum_{n}^{i} BF_i \times (SLA_L)_i \quad (4)$$

where n is the species richness (number of species) of the community, and BF_i is the ratio of aboveground biomass of the ith species to the total aboveground biomass of the community. LA_L and SLA_L represent values of LA and SLA at leaf scale. Aboveground biomass of each species was obtained by directly weighing dried plant tissue per quadrat. Community $1/\triangle^{18}O$ was used in this study as a proxy for canopy conductance (G_s) (Cabrera *et al.* 2021; Hirl *et al.* 2021). We also derived G_s from gross primary productivity and community ratio of intercellular to atmospheric CO_2 partial pressure (Cabrera-Bosquet *et al.* 2011).

2.4 Auxiliary dataset

Climate variables were obtained from the standard (19) WorldClim Bioclimatic variables for WorldClim version 2 (1 km^2) (https://www.worldclim.org/) (Fick and Hijmans 2017). The growing season (April to October) and annual mean air temperature, maximum temperature, actual water vapor pressure, and cumulative precipitation were calculated from monthly values. Vapor pressure deficit (VPD) was calculated from actual water vapor pressure and temperature (Grossiord *et al.* 2020). Aridity index (=1-MAP/potential evapotranspiration) was obtained from the CGIAR-CSI (https://cgiarcsi.community). Solar radiation was derived from "A dataset of reconstructed photosynthetically active radiation in China (1961–2014)" (Liu *et al.* 2017). Soil moisture content within the top 10 cm depth was obtained from remote-sensing-based surface soil moisture (RSSSM) dataset at 0.1° spatial resolution (Chen *et al.* 2021), and approximately 10-day temporal resolution.

2.5 Statistical analysis

Linear regressions were used to describe the patterns of climatic variables and G_s along an aridity gradient (Matlab, Version 2018b). Differences in climate variables among the three transects were tested with a one-way ANOVA with Duncan's post

hoc multiple comparisons (SPSS, Chicago, IL, USA). To explore bivariate relationships between each of our hypothesized drivers (water variables and plant attributes) and G_s, we conducted Pearson correlation analyses using IBM SPSS 20 software (SPSS, Chicago, IL). We tested the differences in slopes and intercepts of linear regression between G_s and aridity using standardized major axis (SMA) regression fitting (Wright *et al.*, 2006) (R Core Team 2012). To determine the interactive effects of climate variables and plant properties on variability in G_s along an aridity gradient, we fitted structural equation models using the "lavaan" package in R statistical program (R Core Team 2012) based on the current knowledge of the interactive relationships between climate variables, plant properties, and G_s (Fig.S3-4). We chose the final models with high-fit statistics: comparative fit index >0.95, standardized root mean square residual < 0.08, and p-value > 0.8.

3 Results

3.1 Variability in $1/\triangle^{18}O$ along aridity gradients

Bivariate linear regression between community $1/\triangle^{18}O$ and aridity showed that $1/\triangle^{18}O$ decreased linearly with increasing aridity within transects (Fig.2a). The standardized major axis (SMA) regression fitting demonstrated that intercepts of SMA were significantly different from each other ($P<0.05$), while the slopes were not ($P>0.05$). The order of the intercepts was Loess Plateau (LP) > Inner Mongolia (MP) > Tibetan Plateau (TP) ($P<0.05$, Table S4). The intercepts of SMA significantly decreased with increasing growing season solar radiation (SR) ($P<0.05$) (Fig.3b) and significantly increased with increasing growing season temperature ($P<0.05$) (Fig.3c). Significant differences in community $1/\triangle^{18}O$ were found among transects ($P<0.001$), and the order was LP>MP>TP (Fig.2b).

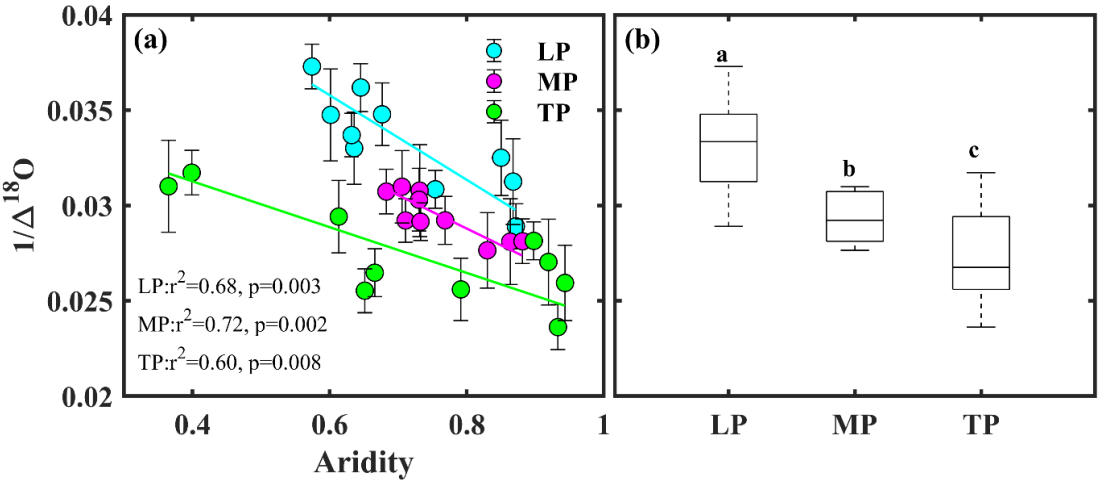

Figure 2. Patterns of community $1/\triangle^{18}O$ (a) along an aridity gradient within transects, and among (b) transects. Different letters indicate significant differences ($P < 0.001$) among transects. $\triangle^{18}O$, ^{18}O enrichment above source water of leaf organic matter; LP, Loess Plateau; MP, Inner Mongolia Plateau; TP, Tibetan Plateau.

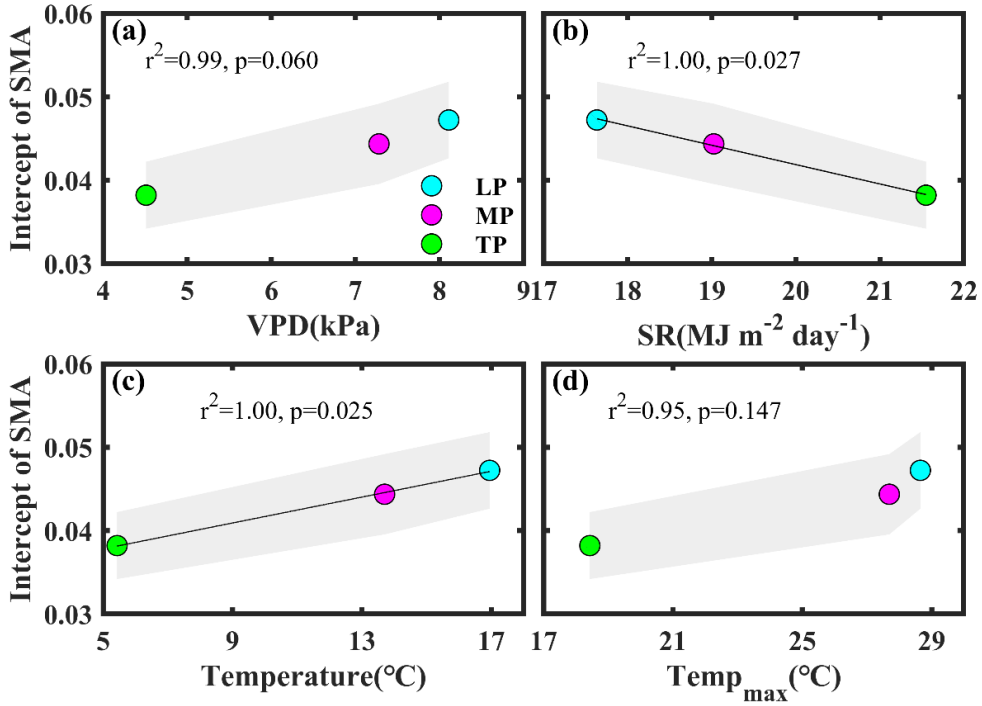

Figure 3. Patterns of the intercept obtained from standardized major axis analysis (SMA) among transects. VPD, vapor pressure deficit; SR, solar radiation; $Temp_{max}$, maximum temperature. LP, Loess Plateau; MP, Inner Mongolia Plateau; TP, Tibetan Plateau. Shaded area represents the 95% confidence interval of the SMA intercept.

3.2 Effects of SM and VPD on the variability in community $1/\triangle^{18}O$

Pearson correlation analysis showed that community $1/\triangle^{18}O$ was positively correlated with soil moisture (SM) along aridity gradients within three transects ($P<0.05$, Table 1), while a significant relationship between $1/\triangle^{18}O$ and VPD was observed only in TP ($P<0.01$). Partial correlation analyses showed that $1/\triangle^{18}O$ was not related to SM ($P > 0.05$) after controlling for VPD, indicating that variability in $1/\triangle^{18}O$ in TP was mainly determined by VPD. SR exhibited negative correlations with $1/\triangle^{18}O$ in all three Plateaus ($P<0.05$). Both mean temperature ($Temp_{mean}$) and $Temp_{max}$ were significantly and positively correlated with $1/\triangle^{18}O$ in LP ($P<0.05$), but negatively in TP ($P<0.05$). However, there were no significant correlations between either $Temp_{mean}$ or $Temp_{max}$ and $1/\triangle^{18}O$ in MP ($P>0.05$). Positive correlations were found between $1/\triangle^{18}O$ and leaf area (LA) in LP and MP ($P<0.05$), and negative between $1/\triangle^{18}O$ and specific leaf area (SLA) in TP ($P<0.05$).

Table 1 Pearson's correlation coefficients among community $1/\triangle^{18}O$ and environmental factors and plant properties.

	Loess Plateau	Inner Mongolia Plateau	Tibetan Plateau
Aridity	-0.848**	-0.843**	-0.773**
SM	0.719*	0.707*	0.659*
VPD	-0.554	-0.384	-0.912**
SR	-0.639*	-0.728*	-0.850**
$Temp_{mean}$	0.641*	0.303	-0.670*
$Temp_{max}$	0.678*	0.038	-0.852**
LA	0.757*	0.913**	0.610
SLA	-0.519	-0.576	-0.648*

**, P<0.01; *, P<0.05. SM, soil moisture; VPD, vapor pressure deficit; SR, total solar radiation; $Temp_{mean}$, mean temperature; $Temp_{max}$, maximum temperature; LA, log-transformed leaf area; SLA, log-transformed specific leaf area.

200

The interactive effects of environmental factors (Table 1) on community $1/\triangle^{18}O$ within transects were determined with structural equation models (SEMs) (Fig.4a-c). SR, acting via SM, exhibited negative effects on $1/\triangle^{18}O$ in LP (standardized path coefficient of indirect effect [SPCI]= -0.52) (Fig.4a). $Temp_{max}$ did not exert a significant effect on $1/\triangle^{18}O$ in LP (P>0.05). SR exhibited a negative indirect effect on $1/\triangle^{18}O$ via SM in MP (SPCI = -0.53) (Fig.4b). The negative indirect effects of SR (SPCI = -0.49) and $Temp_{max}$ (SPCI = -0.45) on $1/\triangle^{18}O$ via VPD in TP were similar (Fig.4c).

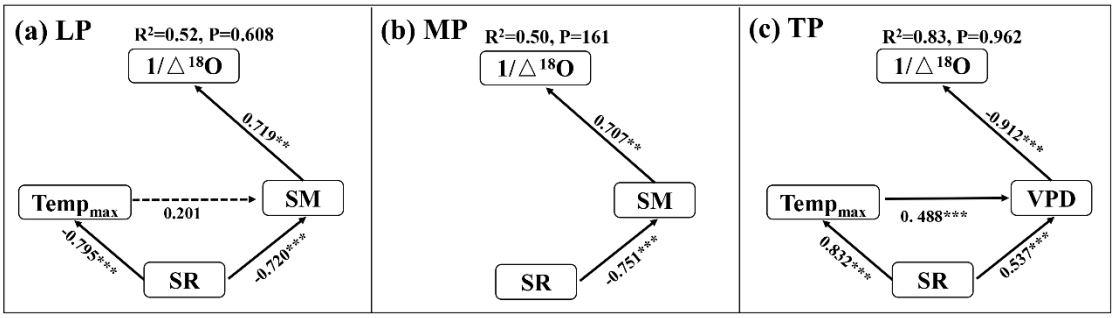

Figure 4. Structural equation models of abiotic factors explaining community $1/\triangle^{18}O$ in Loess Plateau (LP) (a), Inner Mongolia Plateau (MP) (b) and Tibetan Plateau (TP) (c). $\triangle^{18}O$, ^{18}O enrichment above source water of leaf organic matter; $Temp_{max}$: maximum temperature; SR, solar radiation; SM, soil moisture; VPD, vapor pressure deficit. Solid and dashed arrows represent significant and non-significant relationships in a fitted SEM, respectively. ***, P<0.001; **, P<0.01; *, P<0.05.

3.3 Interactive effects of abiotic and biotic factors on the variability in 1/△^{18}O

When community LA and SLA were incorporated into the SEM, community 1/△^{18}O prediction significantly improved in LP and MP, but there was no change in TP (Fig.5). In particular, LA had a positive effect on 1/△^{18}O in LP, and its effect [SPC=0.517] was slightly larger than that of SM [SPC=0.430] (Fig.5a). LA exhibited a positive direct effect on 1/△^{18}O in MP, while the effect of SM was not statistically significant (Fig.5b). However, SLA did not directly affect 1/△^{18}O in TP (P>0.05) (Fig.5c).

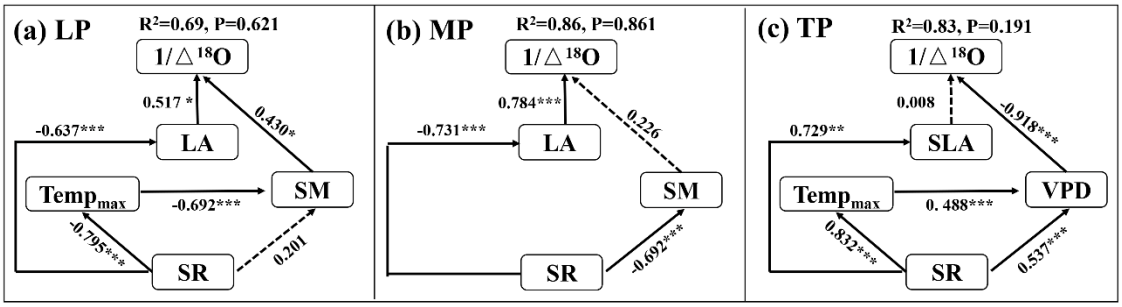

Figure 5. Structural equation models of abiotic and biotic factors explaining community 1/△^{18}O in Loess Plateau (LP) (a), Inner Mongolia Plateau (MP) (b) and Tibetan Plateau (TP) (c). △^{18}O, ^{18}O enrichment above source water of leaf organic matter; $Temp_{max}$: maximum temperature; SR, solar radiation; SM, soil moisture; VPD, vapor pressure deficit. LA, log-transformed leaf area; SLA, log-transformed specific leaf area. Solid and dashed arrows represent significant and non-significant relationships in a fitted SEM, respectively. ***, P<0.001; **, P<0.01; *, P<0.05.

4 Discussion

4.1 Radiation and temperature regulates variability in canopy conductance within transects via drought stress

Community △^{18}O in this study was relatively high (from a low of 26.8‰ in Loess Plateau (LP) to a high of 42.4‰ in Tibetan Plateau (TP)) (Fig.2a, Table S1). A previous study conducted in a temperate grassland (mean annual precipitation was 753 mm) reported △^{18}O of 28.2~30.53‰ (Hirl et al. 2021). This indicated that the canopy conductance (G_s), presented by community 1/△^{18}O, was relatively low in this study, and community reduces G_s in response to drought stress.

The decreasing G_s with aridity within transects was mainly due to drought stress, coupled with effects of high solar radiation or/and temperature. However, the relative roles of soil moisture (SM) and vapor pressure deficit (VPD) in restricting G_s along an aridity gradient were different across the three transects (Table 1). In this study, we found that the variability in G_s was limited by SM in LP and MP, and mainly by VPD in TP. In addition, a global meta-analysis demonstrated that ecosystem conductance was mainly limited by low SM in xeric sites, and by VPD in mesic sites (Novick *et al.* 2016). This

indicated that drought stress may be primarily controlled by SM in LP and MP, but may be limited by both SM and VPD in TP. An eddy covariance study conducted in TP demonstrated that gross primary productivity (GPP) in the growing season was significantly limited by SM and VPD, however, the accumulated GPP was primarily determined by SM (Xu *et al.* 2021b). This may be because the dominant factors of drought stress differ for different spatial and temporal scales.

Solar radiation and temperature regulated variability in G_s within transect via drought stress (Fig.4). Solar radiation exhibited consistently negative effects on G_s because it increased with increasing aridity within the three transects (Fig.1h, Table S1). These results were consistent with those of Fu et al. (2006), who demonstrated that the net CO_2 exchange in grasslands in MP and shrublands in TP was significantly reduced by high solar radiation. In this study, solar radiation exhibited a negative effect on G_s via drought stressors (Fig.4 a-c). On one hand, increasing solar radiation would decrease SM by increasing energy partitioning into evaporation and transpiration (Zhang *et al.* 2019). In fact, solar radiation had negative effects on SM in the three transects in this study (Table S5). On the other hand, increasing solar radiation can increase VPD by increasing temperatures (Grossiord *et al.* 2020). However, a positive relationship between temperature and VPD was observed only in TP (Table S2).

The drought stress on G_s within transect was exacerbated by higher temperatures in TP (Fig.4c). In TP, temperature increased with increasing aridity (Table S1), and was negatively related to SM and positively to VPD (Table S5, Fig.4c). As with solar radiation, increases in temperature tend to increase evaporation and transpiration, ultimately reducing SM, while VPD always increases with increasing temperatures (Grossiord *et al.* 2020; Oren *et al.* 1999). Consequently, increasing temperatures exacerbate soil and atmospheric drought, ultimately reducing G_s along an aridity gradient in TP. However, temperature exhibited negative correlations with community $1/\triangle^{18}O$ in LP, while it did not exhibit significant effects on community $1/\triangle^{18}O$ in the SEM models (Fig.4a). The reason may be that temperature was significantly correlated with SM in LP (Table S5).

4.2 Interacting effects of abiotic and biotic factors on the variability in canopy conductance within transects

Our results indicated that solar radiation and temperature indirectly regulated variability in G_s along an aridity gradient within transects through leaf morphological properties. Including leaf area (LA) increased the percentage of explained variability in G_s by 17 and 36% in LP and MP, respectively (Fig.5a-b), over models which excluded plant variables. This highlighted the need to integrate plant properties related to light capture and heat exchange when examining spatial variability in Gs. To the best of our knowledge, this study was the first in which leaf morphological properties were included to quantify the relative contributions of climatic and vegetation variables on G_s. Specifically, solar radiation exhibited negative effects on G_s via LA in LP and MP (Fig.5a-b). Kang et al. (2021) noted that plants tend to balance light capture with damage from high solar radiation. Solar radiation increased with increasing aridity in LP and MP (Table S5). Consequently, our results demonstrated that communities in LP and MP prevail by reducing LA to avoid damage at the expense of light capture.

Our earlier preliminary study demonstrated that g_s at species level was significantly affected by LA in TP at species level (Wang and Wen 2022a). However, the effect of community LA on G_s was weak (P=0.061) (Fig.S5a), and variability in G_s along an aridity gradient was controlled by specific leaf area (SLA) (Table 1, Fig.S5b). This highlighted the difference in biological drivers of g_s at leaf and canopy scales. Contrary to the results from the dry grassland species in Mediterranean (Prieto *et al.* 2018) and karst communities in subtropical regions (Wang *et al.* 2021a), community $1/\triangle^{18}O$ significantly decreased with SLA in this study (Table S1, Fig.S5). This indicated that the traditional leaf economic spectrum theory may not be supported at community level in TP due to multiple environmental stressors. SLA generally decreases with increasing solar radiation, and increases with temperature and water availability (Poorter *et al.* 2009). In this study, communmnity SLA was negatively related to soil moisture, and positively related to maximum temperature (Table S5) indicating that changes in commumnity SLA were mainly controlled by maximum temperature. However, the direct effect of SLA on G_s in the structural equation was not significant (Fig.5c). This effect may be obscured by drought stress.

4.3 Differences in canopy conductance among transects

Significant differences in community $1/\triangle^{18}O$ for a given level of aridity were found among transects (Fig.2a). Among transects, only differences in VPD, solar radiation and temperature were significant (P>0.05) (Fig.1 and Fig.S1). In general, plants decrease their g_s at species level to respond to increasing VPD (Grossiord *et al.* 2020). The intercept of linear regression between aridity and community $1/\triangle^{18}O$ decreased with decreasing VPD among transects (P>0.05) (Fig.3a). This indicated that the difference in VPD was not a contributor to the difference in G_s among transects.

The differences in G_s among transects may be attributed to the direct effects of solar radiation and temperature on G_s and photosynthesis (Yu *et al.* 2002). Solar radiation exhibited a negative effect on the intercept of linear regression between aridity and community $1/\triangle^{18}O$ among transects (P<0.05) (Fig.3b). Excess ultraviolet-B radiation (Duan *et al.* 2008), insufficient thermal dissipation, and enhanced photorespiration under high solar radiation (Cui *et al.* 2003) can decrease photosynthesis, ultimately reducing g_s at species level. For example, Yu et al. (2012) observed that photosynthesis in wheat in TP at leaf level was lower than that in North China Plain due to the high solar radiation in TP.

Transect with the low temperature exhibited a low intercept of linear regression between aridity and community $1/\triangle^{18}O$ (Fig.3c), indicating that G_s differences among transects were also inhibited by low temperature. Generally, photosynthesis and G_s increased with temperature below the optimum temperature (Xu *et al.* 2021a). For example, the rate of photosynthesis in what was lower in a cold than in a warm environment (Yu *et al.* 2002).

4.4 Using community-weighted $1/\triangle^{18}O$ as an indicator of canopy conductance

Positive relationships between community $1/\triangle^{18}O$ and G_s derived from GPP (Cabrera-Bosquet *et al.* 2011) (LP: r^2=68, p=0.003; MP: r^2=0.76, p=0.001; TP: r^2 = 0.67, p = 0.004) indicated that community $1/\triangle^{18}O$ is an effective indicator of the

growing season-integrated G_s along aridity gradients (Cabrera *et al.* 2021; Hirl *et al.* 2021). However, caution is advised for studies at large scales (Moreno-Gutierrez *et al.* 2012; Prieto *et al.* 2018) because leaf $\triangle^{18}O$ was influenced by multiple environmental conditions (e.g., $\delta^{18}O$ of source water, temperature, VPD) (Song *et al.* 2011).

Interspecific differences in rooting and water acquisition depth and phenology among coexisting species can lead to substantial differences in the $\delta^{18}O$ of their water sources (Moreno-Gutierrez *et al.* 2012). Previous studies found that the depth of water uptake of co-occurring species in grasslands commonly occurred in shallow soil layers throughout dry and wet periods (Bachmann et al. 2015; Hirl et al. 2019; Prieto et al. 2018). The differences in water acquisition depth could be ruled out as a major source of interspecific variation in leaf $\delta^{18}O$ in this study (Prieto *et al.* 2018). However, soil evaporation always exhibited increasing trends with increasing aridity, and usually resulted in heavy enrichment in $\delta^{18}O$ in the remaining soil water used by plants (Lyu *et al.* 2021). Longer rainless periods and heavier evaporative enrichment of soil water along the aridity gradient could also contribute to a decreasing trend in community $1/\triangle^{18}O$. Consequently, our results may overestimate the decreasing trend in G_s along the aridity gradient.

The decreasing trend in community $\triangle^{18}O$ along aridity may originate from temperature and VPD through their effects on evaporation and isotopic exchange between water and organic molecules (Barbour and Farquhar 2000; Helliker and Richter 2008; Song *et al.* 2011). For example, the equilibrium fractionation factor for water evaporation is dependent on temperature (Bottinga and Craig 1968). Temperature and VPD gradients between leaf and ambient air influence the evaporative gradient from leaf to air (Helliker and Richter 2008; Song *et al.* 2011). In addition, biochemical ^{18}O-fractionation during cellulose synthesis is sensitive to temperature, and the proportion of oxygen in cellulose derived from source water was humidity-sensitive (Hirl *et al.* 2021).

The potential effects of temperature and VPD on $\triangle^{18}O$ via evaporation and isotopic exchange between water and organic molecules could be ruled out in this study. The growing season temperature variation was small along three transects (LP=3.3 °C, MP=4.9 °C, and TP=3.8 °C) (Table S1). However, community $\triangle^{18}O$ ranged from 3.89‰ in MP to 7.78‰ in LP (Table S1, Fig.2a). Previous studies demonstrated that the sensitivity of temperature to $\triangle^{18}O$ was approximately 0.23‰/°C (Helliker and Richter 2008; Song *et al.* 2011). It seems that the changes in temperature were not a main contributor to the large variability in community $\triangle^{18}O$. Meanwhile, a positive relationship between community $1/\triangle^{18}O$ and temperature was observed in LP ($P<0.05$), and negative between community $1/\triangle^{18}O$ and VPD in TP (Table 1). However, partial correlation analyses showed that community $1/\triangle^{18}O$ was not related to temperature ($P > 0.05$) and VPD after controlling for G_s (data not shown). This indicated that the variability in community $1/\triangle^{18}O$ was mainly determined by G_s.

5 Conclusions

This study highlighted the need to integrate multiple stressors and plant properties when determining spatial variability in G_s, and directly link species-level observations of physiological processes to canopy-level observations of functions at a large spatial scale. Specifically, our results demonstrated that excess radiation and low temperature interacted to exacerbate drought stress impacts on G_s across transects, while solar radiation exacerbated drought stress impacts on G_s within transects. Effects of drought stress on G_s can be mitigated by decreasing temperatures in warm environments, and aggravated by increasing temperatures in cold environments. The primary determinant of drought stress on G_s was soil moisture in LP and MP, and vapor pressure deficit in TP. The ability to predict variability in G_s could be significantly improved by integrating multiple stressors and leaf area in LP and TP, but not in TP due to an overwhelming effect of climate.

Data availability

Data availability. Requests for leaf $\delta^{18}O$ and $\triangle^{18}O$ data should be directed to Xuefa Wen (wenxf@igsnrr.ac.cn). Requests for leaf area and specific leaf area at species level should be directed to Nianpeng He (Henp@igsnrr.ac.cn).

Author contributions

JW and XFW planed and designed the research. JW performed experiments and analyzed data. All authors jointly wrote the manuscript. All authors contributed critically to the drafts and gave final approval for publication.

Competing interests

The authors declare that they have no conflict of interest.

Acknowledgements

We thank the “Functional Trait database of terrestrial ecosystems in China (China_Traits)” for sharing leaf area and specific leaf area data. This work was supported by the National Natural Science Foundation of China (41991234, 32001137).

References

Ahlstrom, A., Raupach, M.R., Schurgers, G., Smith, B., Arneth, A., Jung, M., Reichstein, M., Canadell, J.G., Friedlingstein, P., Jain, A.K., Kato, E., Poulter, B., Sitch, S., Stocker, B.D., Viovy, N., Wang, Y.P., Wiltshire, A., Zaehle, S. and Zeng, N.: The dominant role of semi-arid ecosystems in the trend and variability of the land CO_2 sink, Science, 348, 895-899, 2015.

Bachmann, D., Gockele, A., Ravenek, J.M., Roscher, C., Strecker, T., Weigelt, A. and Buchmann, N.: No Evidence of Complementary Water Use along a Plant Species Richness Gradient in Temperate Experimental Grasslands, PLoS One, 10, 2015.

Barbour, M.: Stable oxygen isotope composition of plant tissue: a review, Functional Plant Biology, 34, 83-94, 2007.

Barbour, M.M. and Farquhar, G.D.: Relative humidity- and ABA-induced variation in carbon and oxygen isotope ratios of cotton leaves, Plant Cell Environ., 23, 473-485, 2000.

Bottinga, Y. and Craig, H.: Oxygen isotope fractionation between CO_2 and water, and the isotopic composition of marine atmospheric CO2, Earth and Planetary Science Letters, 5, 285–295, 1968.

Bowen, G.J., Wassenaar, L.I. and Hobson, K.A.: Global application of stable hydrogen and oxygen isotopes to wildlife forensics, Oecologia, 143, 337-348, 2005.

Buckley, T.N.: How do stomata respond to water status?, New Phytol., 224, 21-36, 2019.

Cabrera-Bosquet, L., Albrizio, R., Nogues, S. and Araus, J.L.: Dual Delta ^{13}C/delta ^{18}O response to water and nitrogen availability and its relationship with yield in field-grown durum wheat, Plant Cell Environ., 34, 418-433, 2011.

Cabrera, J.C.B., Hirl, R.T., Schaeufele, R., Macdonald, A.andSchnyder, H.: Stomatal conductance limited the CO_2 response of grassland in the last century, Bmc Biology, 19, 2021.

Chen, Y., Feng, X. and Fu, B.: An improved global remote-sensing-based surface soil moisture (RSSSM) dataset covering 2003–2018, Earth Syst. Sci. Data, 13, 1-31, 2021.

Costa, A.C., Rezende-Silva, S.L., Megguer, C.A., Moura, L.M.F., Rosa, M. and Silva, A.A.: The effect of irradiance and water restriction on photosynthesis in young jatoba-do-cerrado (Hymenaea stigonocarpa) plants, Photosynthetica, 53, 118-127, 2015.

Cui, X.Y., Tang, Y.H., Gu, S., Nishimura, S., Shi, S.B. and Zhao, X.Q.: Photosynthetic depression in relation to plant architecture in two alpine herbaceous species, Environ. Exp. Bot., 50, 125-135, 2003.

Doupis, G., Chartzoulakis, K.S., Taskos, D. and Patakas, A.: The effects of drought and supplemental UV-B radiation on physiological and biochemical traits of the grapevine cultivar "Soultanina", Oeno One, 54, 2020.

Duan, B.L., Xuan, Z.Y., Zhang, X.L., Korpelainen, H. and Li, C.Y.: Interactions between drought, ABA application and supplemental UV-B in Populus yunnanensis, Physiologia Plantarum, 134, 257-269, 2008.

Farquhar, G., Barbour, M. and Henry, B.: Interpretation of oxygen isotope composition of leaf material Stable isotope: integration of biological, ecological and geochemical processes 27-62, 1998.

Farquhar, G.D., Caemmerer, S.V. and Berry, J.A.: A biochemical-model of photosynthetic CO_2 assimilation in leaves of C3 species, Planta, 149, 78-90, 1980.

Fick, S.E. and Hijmans, R.J.: WorldClim 2: new 1-km spatial resolution climate surfaces for global land areas, International Journal of Climatology, 37, 4302-4315, 2017.

Fu, Y.L., Yu, G.R., Sun, X.M., Li, Y.N., Wen, X.F., Zhang, L.M., Li, Z.Q., Zhao, L. and Hao, Y.B.: Depression of net ecosystem CO_2 exchange in semi-arid Leymus chinensis steppe and alpine shrub, Agric. For. Meteorol., 137, 234-244, 2006.

Fyllas, N.M., Bentley, L.P., Shenkin, A., Asner, G.P., Atkin, O.K., Diaz, S., Enquist, B.J., Farfan-Rios, W., Gloor, E., Guerrieri, R., Huasco, W.H., Ishida, Y., Martin, R.E., Meir, P., Phillips, O., Salinas, N., Silman, M., Weerasinghe, L.K., Zaragoza-Castells, J. and Malhi, Y.: Solar radiation and functional traits explain the decline of forest primary productivity along a tropical elevation gradient, Ecol Lett, 20, 730-740, 2017.

Galmes, J., Medrano, H. and Flexas, J.: Photosynthetic limitations in response to water stress and recovery in Mediterranean plants with different growth forms, New Phytol., 175, 81-93, 2007.

Grossiord, C., Buckley, T.N., Cernusak, L.A., Novick, K.A., Poulter, B., Siegwolf, R.T.W., Sperry, J.S. and McDowell, N.G.: Plant responses to rising vapor pressure deficit, New Phytol., 226, 1550-1566, 2020.

Guerrieri, R., Belmecheri, S., Ollinger, S.V., Asbjornsen, H., Jennings, K., Xiao, J.F., Stocker, B.D., Martin, M., Hollinger, D.Y., Bracho-Garrillo, R., Clark, K., Dore, S., Kolb, T., Munger, J.W., Novick, K. and Richardson, A.D.: Disentangling the role of photosynthesis and stomatal conductance on rising forest water-use efficiency, Proceedings of the National Academy of Sciences of the United States of America, 116, 16909-16914, 2019.

Helliker, B.R. and Richter, S.L.: Subtropical to boreal convergence of tree-leaf temperatures, Nature, 454, 511-514, 2008.

Hirl, R.T., Ogee, J., Ostler, U., Schaufele, R., Cabrera, J.C.B., Zhu, J.J., Schleip, I., Wingate, L. and Schnyder, H.: Temperature-sensitive biochemical O-18-fractionation and humidity-dependent attenuation factor are needed to predict delta O-18 of cellulose from leaf water in a grassland ecosystem, New Phytol., 229, 16, 2021.

Hirl, R.T., Schnyder, H., Ostler, U., Schaufele, R., Schleip, I., Vetter, S.H., Auerswald, K., Cabrera, J.C.B., Wingate, L., Barbour, M.M. and Ogee, J.: The O-18 ecohydrology of a grassland ecosystem - predictions and observations, Hydrol. Earth Syst. Sci., 23, 2581-2600, 2019.

Jarvis, P.G. and McNaughton, K.G.: Stomatal control of transpiration - scaling up from leaf to region, Advances in Ecological Research, 15, 1-49, 1986.

Kang, X.M., Li, Y.A., Zhou, J.Y., Zhang, S.T., Li, C.X., Wang, J.H., Liu, W. and Qi, W.: Response of Leaf Traits of Eastern Qinghai-Tibetan Broad-Leaved Woody Plants to Climatic Factors, Front. Plant Sci., 12, 2021.

Keitel, C., Matzarakis, A., Rennenberg, H.andGessler, A.: Carbon isotopic composition and oxygen isotopic enrichment in phloem and total leaf organic matter of European beech (Fagus sylvatica L.) along a climate gradient, Plant Cell Environ., 29, 1492-1507, 2006.

Kimm, H., Guan, K.Y., Gentine, P., Wu, J., Bernacchi, C.J., Sulman, B.N., Griffis, T.J.andLin, C.J.: Redefining droughts for the US Corn Belt: The dominant role of atmospheric vapor pressure deficit over soil moisture in regulating stomatal behavior of Maize and

Soybean, Agric. For. Meteorol., 287, 2020.
Leuning, R.: A critical-appraisal of a combined stomatal-photosynthesis model for C-3 plants, Plant Cell Environ., 18, 339-355, 1995.
Liu, H., Hu, B., Wang, Y., Liu, G., Tang, L., Ji, D., Bai, Y., Bao, W., Chen, X., Chen, Y., Ding, W., Han, X., He, F., Huang, H., Huang, Z., Li, X., Li, Y., Liu, W., Lin, L., Ouyang, Z., Qin, B., Shen, W., Shen, Y., Su, H., Song, C., Sun, B., Sun, S., Wang, A., Wang, G., Wang, H., Wang, S., Wang, Y., Wei, W., Xie, P., Xie, Z., Yan, X., Zeng, F., Zhang, F., Zhang, Y., Zhang, Y., Zhao, C., Zhao, W., Zhao, X., Zhou, G. and Zhu, B.: Two ultraviolet radiation datasets that cover China, Adv. Atmos. Sci., 34, 805-815, 2017.
Liu, L.B., Gudmundsson, L., Hauser, M., Qin, D.H., Li, S.C. and Seneviratne, S.I.: Soil moisture dominates dryness stress on ecosystem production globally, Nat. Commun., 11, 9, 2020.
Lyu, S.D., Wang, J., Song, X.W. and Wen, X.F.: The relationship of delta D and delta O-18 in surface soil water and its implications for soil evaporation along grass transects of Tibet, Loess, and Inner Mongolia Plateau, J. Hydrol., 600, 2021.
Martin-StPaul, N., Delzon, S. and Cochard, H.e.: Plant resistance to drought depends on timely stomatal closure, Ecol. Lett., 20, 1437–1447, 2017.
Maxwell, T., Silva, L. and Horwath, W.: Integrating effects of species composition and soil properties to predict shifts in montane forest carbon-water relations, Proceedings of the National Academy of Sciences of the United States of America, 115, E4219-E4226, 2018.
Moreno-Gutierrez, C., Dawson, T.E., Nicolas, E. and Querejeta, J.I.: Isotopes reveal contrasting water use strategies among coexisting plant species in a Mediterranean ecosystem, New Phytol., 196, 489-496, 2012.
Novick, K.A., Ficklin, D.L., Stoy, P.C., Williams, C.A., Bohrer, G., Oishi, A.C., Papuga, S.A., Blanken, P.D., Noormets, A., Sulman, B.N., Scott, R.L., Wang, L.X. and Phillips, R.P.: The increasing importance of atmospheric demand for ecosystem water and carbon fluxes, Nat. Clim. Chang., 6, 1023-1027, 2016.
Oren, R., Sperry, J.S., Katul, G.G., Pataki, D.E., Ewers, B.E., Phillips, N. and Schafer, K.V.R.: Survey and synthesis of intra- and interspecific variation in stomatal sensitivity to vapour pressure deficit, Plant Cell Environ., 22, 1515-1526, 1999.
Peguero-Pina, J.J., Vilagrosa, A., Alonso-Forn, D., Ferrio, J.P., Sancho-Knapik, D. and Gil-Pelegrin, E.: Living in Drylands: Functional Adaptations of Trees and Shrubs to Cope with High Temperatures and Water Scarcity, Forests, 11, 2020.
Peppe, D.J., Royer, D.L., Cariglino, B., Oliver, S.Y., Newman, S., Leight, E., Enikolopov, G., Fernandez-Burgos, M., Herrera, F., Adams, J.M., Correa, E., Currano, E.D., Erickson, J.M., Hinojosa, L.F., Hoganson, J.W., Iglesias, A., Jaramillo, C.A., Johnson, K.R., Jordan, G.J., Kraft, N.J.B., Lovelock, E.C., Lusk, C.H., Niinemets, U., Penuelas, J., Rapson, G., Wing, S.L. and Wright, I.J.: Sensitivity of leaf size and shape to climate: global patterns and paleoclimatic applications, New Phytol., 190, 724-739, 2011.
Poorter, H., Niinemets, U., Poorter, L., Wright, I.J. and Villar, R.: Causes and consequences of variation in leaf mass per area (LMA): a meta-analysis, New Phytol., 182, 565-588, 2009.
Prieto, I., Querejeta, J., Segrestin, J., Volaire, F. and Roumet, C.: Leaf carbon and oxygen isotopes are coordinated with the leaf economics spectrum in Mediterranean rangeland species, Funct. Ecol., 32, 612-625, 2018.
Ramirez, D.A., Querejeta, J.I. and Bellot, J.: Bulk leaf delta O-18 and delta C-13 reflect the intensity of intraspecific competition for water in a semi-arid tussock grassland, Plant Cell Environ., 32, 1346-1356, 2009.
Seneviratne, S.I., Corti, T., Davin, E.L., Hirschi, M., Jaeger, E.B., Lehner, I., Orlowsky, B. and Teuling, A.J.: Investigating soil moisture–climate interactions in a changing climate: A review, Earth-Sci. Rev., 99, 125–161, 2010.
Song, X., Barbour, M.M., Saurer, M. and Helliker, B.R.: Examining the large-scale convergence of photosynthesis-weighted tree leaf tem pe analysis of multiple data sets, New Phytol., 192, 912-924, 2011.
Wang, J. and Wen, X.F.: Divergence and conservative of stomatal conductance in coexisting species in response to climatic stress in Tibetan Plateau, Ecol. Indic., 138, 108843, 2022a.
Wang, J. and Wen, X.F.: Increasing relative abundance of C4 plants mitigates a dryness-stress effect on gross primary productivity along an aridity gradient in grassland ecosystems, Plant Soil, 2022b.
Wang, J. and Wen, X.: Limiting resource and leaf functional traits jointly determine distribution patterns of leaf intrinsic water use efficiency along aridity gradients, Front. Plant Sci., 13, 2022c.
Wang, J., Wen, X.F., Lyu, S. and Guo, Q.J.: Soil properties mediate ecosystem intrinsic water use efficiency and stomatal conductance via taxonomic diversity and leaf economic spectrum, Sci. Total Environ., 783, 2021a.
Wang, J., Wen, X.F., Lyu, S.D. and Guo, Q.J.: Transition in multi-dimensional leaf traits and their controls on water use strategies of co-occurring species along a soil limiting-resource gradient, Ecol. Indic., 128, 2021b.
Wright, I.J., Dong, N., Maire, V., Prentice, I.C., Westoby, M., Diaz, S., Gallagher, R.V., Jacobs, B.F., Kooyman, R., Law, E.A., Leishman, M.R., Niinemets, U., Reich, P.B., Sack, L., Villar, R., Wang, H. and Wilf, P.: Global climatic drivers of leaf size, Science, 357, 917-921, 2017.
Wright, I.J., Reich, P.B., Westoby, M., Ackerly, D.D., Baruch, Z., Bongers, F., Cavender-Bares, J., Chapin, T., Cornelissen, J.H.C., Diemer, M., Flexas, J., Garnier, E., Groom, P.K., Gulias, J., Hikosaka, K., Lamont, B.B., Lee, T., Lee, W., Lusk, C., Midgley, J.J., Navas, M.L., Niinemets, U., Oleksyn, J., Osada, N., Poorter, H., Poot, P., Prior, L., Pyankov, V.I., Roumet, C., Thomas, S.C., Tjoelker, M.G., Veneklaas, E.J. and Villar, R.: The worldwide leaf economics spectrum, Nature, 428, 821-827, 2004.
Xu, J.M., Wu, B.F., Ryu, D., Yan, N.N., Zhu, W.W. and Ma, Z.H.: A canopy conductance model with temporal physiological and

environmental factors, Sci. Total Environ., 791, 2021a.
Xu, M.J., Zhang, T., Zhang, Y.J., Chen, N., Zhu, J.T., He, Y.T., Zhao, T.T. and Yu, G.R.: Drought limits alpine meadow productivity in northern Tibet, Agric. For. Meteorol., 303, 2021b.
Yao, J.Y., Liu, H.P., Huang, J.P., Gao, Z.M., Wang, G.Y., Li, D., Yu, H.P. and Chen, X.Y.: Accelerated dryland expansion regulates future variability in dryland gross primary production, Nat. Commun., 11, 10, 2020.
Yu, Q., Liu, Y., Liu, J. and Wang, T.: Simulation of leaf photosynthesis of winter wheat on Tibetan Plateau and in North China Plain, Ecol. Model., 155, 205-216, 2002.
Zeuthen, J., Mikkelsen, T.N., PaludanMuller, G. and RoPoulsen, H.: Effects of increased UV-B radiation and elevated levels of tropospheric ozone on physiological processes in European beech (Fagus sylvatica), Physiologia Plantarum, 100, 281-290, 1997.
Zhang, T., Shen, S. and Cheng, C.X.: Impact of radiations on the long-range correlation of soil moisture: A case study of the A'rou superstation in the Heihe River Basin, Journal of Geographical Sciences, 29, 1491-1506, 2019.